Atmos. Meas. Tech. Discuss., 8, 7511–7533, 2015
www.atmos-meas-tech-discuss.net/8/7511/2015/
doi:10.5194/amtd-8-7511-2015

Atmospheric Measurement Techniques Discussions
Open Access

The Outdoor Dust Information Node (ODIN) – development and performance assessment of a low cost ambient dust sensor

G. Olivares and S. Edwards

National Institute of Water and Atmospheric Research (NIWA), 41 Market Place, Auckland Central 1010, Auckland, New Zealand

Received: 15 June 2015 – Accepted: 30 June 2015 – Published: 22 July 2015

Correspondence to: G. Olivares (gustavo.olivares@niwa.co.nz)

Published by Copernicus Publications on behalf of the European Geosciences Union.

Abstract

The large gradients in air quality expected in urban areas present a significant challenge to standard measurement technologies. Small, low-cost devices have been developing rapidly in recent years and have the potential to improve the spatial coverage of traditional air quality measurements. Here we present the first version of the Outdoor Dust Information Node (ODIN) as well as the results of the first real-world measurements. The lab tests indicate that the Sharp dust sensor used in the ODIN presents a stable baseline response only slightly affected by ambient temperature. The field tests indicate that ODIN data can be used to estimate hourly and daily $PM_{2.5}$ concentrations after appropriate temperature and baseline corrections are applied. The ODIN seems suitable for campaign deployments complementing more traditional measurements.

1 Introduction

Global estimates indicate that between 70–90 % of the population is exposed to average annual $PM_{2.5}$ concentrations that exceed the World Health Organization Air Quality Guideline of 10 $\mu g\,m^{-3}$ (annual average). This translates into between 2.2 and 7 million premature deaths $year^{-1}$ worldwide (Brauer et al., 2012; Lim et al., 2012).

A significant source of uncertainty in these estimates is the spatial representativeness of the measurements used to generate them. The cost of installing and operating air quality monitoring stations means that a small number of measurements are used to represent extensive geographical areas (Wilson et al., 2005; Asian Development Bank, 2014). This is particularly relevant in urban areas where large gradients are expected in the concentration of pollutants especially in areas with large density of sources. These gradients can not be resolved if the spatial coverage of the measurements is inadequate (Chow et al., 2002; Holstius et al., 2014; Wilson et al., 2005).

Also, capturing accurate data to assess personal exposure to air pollution is critical when dealing with human health effects (McKone et al., 2008; Snyder et al., 2013).

AMTD
8, 7511–7533, 2015

Determining exposure in both time and space is challenging as individual behaviour affects daily and long term exposure to air pollution (Wilson et al., 2005). Therefore, health effect studies require accurate, spatially and temporally resolved air quality data. Epidemiological studies often use ambient concentrations at a city level as a proxy for exposure. The spatial and temporal resolution of reported data sets means they are unlikely to adequately reflect individual pollution exposure (Chow et al., 2002). Modelling can partially compensate for the lack of spatial resolution, but in regions with complex topography and meteorology or unevenly distributed and poorly characterised emission sources, model accuracy is constrained (Wilson et al., 2005).

The spatial and temporal resolution of air pollution data sets could be improved by deploying additional sensors to supplement existing monitoring networks. Where previously the cost of doing so was prohibitive, rapid advances in technology in recent years have seen increasing numbers of low cost air pollution sensors available. Individuals and non-regulatory groups have seized the opportunity and developed citizen science initiatives to monitor their local air quality (Egg, 2014; Hart and Martinez, 2006; Smith and Clark, 2013; SPECK, 2015).

Whilst low-cost sensors have increased the accessibility of air pollution data to the general public, the sensors are not without limitations. Instruments used for regulatory monitoring must meet high standards of precision, accuracy, comparability and traceability (Wang and Brauer, 2014) whereas low cost sensors are often provided without calibration information and have either not been characterised under ambient conditions or tested only for a limited time leaving questions on their long term reliability (Snyder et al., 2013). This is not necessarily a problem if the purpose of the measurements is commensurate with the capabilities of the sensors. For example, in some cases qualitative information indicating an increase or decrease of pollutant levels might be sufficient. However, in order to derive quantitative information from each sensor response, some level of evaluation against more robust monitors is required. This is likely to result in site specific calibrations, given the variable nature of aerosol

AMTD
8, 7511–7533, 2015

composition. To date very few low-cost pollution sensors have been evaluated against compliance monitoring instruments (Holstius et al., 2014; Williams et al., 2014).

We have made some progress in the use of low cost sensors for the assessment of personal pollution exposure with the development of the Particles, Activity and Context Monitoring Autonomous Node (PACMAN) for indoor exposure studies (Olivares et al., 2013). In this work we describe the development of the outdoor counterpart of PACMAN the Outdoor Dust Information Node (ODIN), a new, low-cost, battery powered sensor package to monitor outdoor particulate concentrations. We also explore the performance of the dust sensor at the heart of ODIN and PACMAN in terms of baseline stability. Finally, we present results of the first field tests of the ODIN co-located with traditional standard instrumentation at a regulatory monitoring site in Christchurch, New Zealand. These tests indicate that the ODIN is able to capture $PM_{2.5}$ concentrations once suitable corrections are applied which make it a viable instrument to measure PM in combustion dominated areas complementing traditional measurements.

2 Methods

2.1 ODIN

The Outdoor Dust Information Node (ODIN) was developed leveraging on the extensive open source hardware and software communities using readily available components. In very broad terms, the ODIN is a set of sensors that are integrated by a microcontroller that logs the data. Figure 1 shows a diagram of the operation of ODIN and a view of the internal layout of the device. Power is drawn from either the battery or the solar panel depending on the sunshine. To maximize the battery life, the ODIN uses its microcontroller's *sleep* mode and only wakes up to take a single measurement every minute.The sensors feed information to the microcontroller which in turn saves it to the memory card. The electric design files are available from Olivares and Edwards (2014) and the detail of the components is as follow.

AMTD
8, 7511–7533, 2015

G. Olivares and S. Edwards

- *Dust sensor*: the Sharp Optical Dust Sensor GP2Y1010AU0F was selected because of its low power consumption (SHARP, 2015).The basic measurement principle of this sensor is infra-red light scattering. An infra-red light emitting diode (IRLED) and a photodetector (PD) are arranged 90° to each other around the sensing volume. The particles in the sensing volume scatter the light from the IRLED which is measured by the PD. This sensor requires 5–7 Vdc to operate and outputs a 0–3 Vdc signal proportional to the total dust mass measured. The operation of this sensor is as a 10 ms sampling cycle consisting of a high phase of 0.32 ms and a low phase of 9.68 ms. A single measurement is taken 0.28 ms into the high phase (SHARP, 2015). To smooth the output of this sensor, the microcontroller takes 100 samples of 10 ms each and records their average.

  Note that the dust sensor does not have a defined measurement size range but that the upper and lower cut off sizes are controlled by the sensitivity of the internal amplifying circuit. It is expected that this circuit has significant inter-instrument variability as well as its response to depend on the type of aerosol sampled.

- *Temperature and relative humidity*: the AM2302 temperature-humidity sensor from AOSONG was selected for its size, power consumption and ease of interface. According to the manufacturers, the AM2302 is accurate to within 2 % RH and 0.5 °C and it is able to operate in a wide range of conditions (AOSONG, 2015).

- *Microcontroller*: Sparkfun's Arduino Pro Mini (Sparkfun, 2014) based on the ATMega328 microcontroller was selected primarily because of its ease of use and the programming libraries available for the Arduino system. The firmware used on this microcontroller is available in the project's GitHub repository (Olivares and Edwards, 2014).

- *Memory*: a 2 GB micro SD card is used to log the data. Adafruit's micro SD card adapter board (Adafruit, 2014) was used to interface with the microcontroller. The files created by the units are labelled as YYYYMMDD.TXT, e.g. "20120520.TXT" corresponds to the file for the 20 May 2012.

- *Clock*: the DS3231 based temperature compensated RTC *Chronodot v2.0* (Macetech, 2013) was used to keep track of time. This component is documented to have a drift smaller than one minute per year. A specific library was used to communicate with this component (Maks, 2012).
- *Power*: a lithium ion polymer battery pack (3.7 V) delivers the power required for the unit. A 6 Ah battery is capable of powering the system for six weeks. A solar panel was added to the design which under ideal conditions of sunshine, is capable of powering the system as well as recharging the battery for long term deployments. Unfortunately the chosen combination of solar panel and charging circuit was unable to recover the battery so in future revisions a new solution will be tested.

Figure 1 also shows the internal layout of the ODIN. As the ODIN is a passive instrument, i.e. there is no forced air sample, the dust sensor is located against the wall of the enclosure with its opening directly towards the outside of the instrument, protected by a rain shield and a coarse metal mesh.

The cost of the materials for the prototype ODIN is less than USD 300 (June 2015) and each unit takes about three hours to put together.

2.2 Deployments

Several short deployments were used to capture the data presented here. The first one was aimed at characterise the zero response of the dust sensor at the heart of the ODIN. Eight Sharp dust sensors were set up in a custom made, sealed and uninsulated enclosure and placed in a controlled environment for five days at a temperature of $22 \pm 1\,^{\circ}$C and a relative humidity of $50 \pm 5\,\%$. Following this deployment, the same eight units were placed outdoors in the same sealed container but exposed to sunshine. The sensors were subject to temperatures ranging from 6 to 26 °C. More than 4000 records (66 h) were obtained.

AMTD
8, 7511–7533, 2015

To evaluate the response of the ODIN to woodsmoke and assess its performance against standard air quality instrumentation, one unit (*ODIN_01*) was located at Environment Canterbury's[1] air quality monitoring site at Coles Place (−43.511236° S; 172.633687° W) between the 24 July and the 14 August 2014. The unit was attached to the meteorological mast at the same height as the inlets for the PM_{10} and $PM_{2.5}$ instruments at the site (Fig. 2). The data were manually downloaded from the internal memory at the end of the test period.

Data from the air quality monitoring station were obtained from Environment Canterbury. These data were provided before the normal QA process as 60 min moving average, every 10 min of, PM_{10}, $PM_{2.5}$ measured by a TEOM-FDMS instrument, wind speed and direction and air temperature. The details of these measurements are described by Aberkane et al. (2010).

2.3 Data analysis

All the data analysis was done using R Team (2014) and the Openair R package (Carslaw and Ropkins, 2012). The raw data are available from Olivares (2015a) and the analysis scripts are available from Olivares (2015b).

The baseline of each instrument was obtained by averaging all the measurements taken during the temperature controlled baseline deployment described above. This baseline was then subtracted from the raw measurements to obtain the *baseline corrected* signal. The temperature response of the sensors was estimated using data from the variable temperature baseline deployment. A linear regression between the *baseline corrected* signal and the ambient temperature in the enclosure was performed to describe the effect of ambient temperature on the response of the Sharp dust sensors.

For the co-location deployment the data analysis included the following: we first removed baseline drift, then corrected for temperature effects and then found the calibration coefficients to approximate $PM_{2.5}$.

[1]http://ecan.govt.nz

AMTD
8, 7511–7533, 2015

More in detail, the baseline drift was estimated from the linear trend of the raw response from ODIN. This baseline was subtracted from the raw ODIN output.

Then, a temperature correction was applied by first finding the linear regression between the de-trended ODIN signal and the instrument temperature. This was done by considering only data above 10 °C. Figure 3 shows that above 10 °C the temperature effect dominates the ODIN response. The data were then corrected by subtracting the linear regression with the temperature from the de-trended ODIN output.

To obtain the correction coefficients to estimate $PM_{2.5}$, this de-trended and temperature corrected ODIN signal was used in a linear regression with $PM_{2.5}$ as the dependent variable and the ODIN signal. To explore the stability of this correction, the linear regression was performed on the first 1/3 of the data while the error estimate (RMSE) was calculated using the whole dataset.

3 Results

3.1 Dust sensor behaviour

Table 1 shows the results of the baseline test for the eight sensors tested and highlights the inter-instrument variability for the Sharp dust sensor with the range of baselines between 0.24 to 28 mV. For each sensor, the standard deviation of the baseline estimate suggests a relatively stable baseline for the sensors tested.

In our previous work with similar sensors we found a linear relationship between the baseline response of the dust sensor and ambient temperature in field deployments (Olivares et al., 2013). Our original hypothesis was that this interference by temperature was a property of the sensor so, as described above, we placed several units in a clean environment exposed to a range of temperatures.

If the effect of ambient temperature on the Sharp dust sensor readings was related to the sensor itself we would expect that there would be a significant increase in their baseline response in warmer temperatures even when placed in a clean environment.

AMTD
8, 7511–7533, 2015

As shown in Fig. 4, ambient temperature appears to change the response of the sensors by around 0.3 mV for every 1 °C. This, however is a much weaker response to temperature than what is found when using the sensor as part of the ODIN. Table 2 shows that the temperature correction applied to the ambient data is of 4.4 mV for every 1 °C. This suggests that the impact of temperature on the response from the Sharp dust sensor is dominated by impacts on the aerosol instead of being a property of the devices. However, future tests will further explore this behaviour.

3.2 ODIN's performance evaluation

Figure 5 shows that the raw ODIN data show a significant baseline drift and they only capture a small fraction of the features observed in the $PM_{2.5}$ time series. The baseline correction showed a significant drift of almost −30 % during the deployment (Table 2). After removing the baseline drift, the temperature correction was estimated as 4.4 $mV\,°C^{-1}$ (Table 2) which, as noted above, is significantly higher than what was obtained in clean conditions but similar to what was observed by our group in a previous work (Olivares et al., 2013).

Table 2 shows that, after applying the baseline and temperature corrections, a calibration factor of 0.6 and an offset of 19 $\mu g\,m^{-3}$ is sufficient for the ODIN data to capture most of the variability of $PM_{2.5}$. Figure 6 shows that the corrected ODIN data captured both the timing and intensity of all the high concentration events observed in the $PM_{2.5}$ data. However, for $PM_{2.5}$ concentrations below 25 $\mu g\,m^{-3}$ the scatter plot shows a less defined relationship between ODIN and $PM_{2.5}$.

Figure 6 also shows that the correction calculated for the beginning of the deployment significantly overestimates the low concentrations observed towards the end of the dataset. This could be due to a residual baseline drift not accounted for by the method used but it does not seem to affect the fit for the higher concentrations.

Finally, and to evaluate the behaviour of the ODIN's inlet, we compared the error in the ODIN estimate ($PM_{2.5}$ – ODIN) with the observed wind speed and direction. Figure 7 shows that the error is uniform with wind direction but has a small negative trend

AMTD
8, 7511–7533, 2015

with wind speed. This difference in higher wind speeds could be related to a different source mix than in low wind speeds which typically occur during night time (Aberkane et al., 2010). However, $PM_{2.5}$ concentrations are generally lower in high wind speeds which, as indicated before, is closer to the detection limit of the Sharp dust sensor.

4 Conclusions

The small, low-cost dust monitor ODIN, based on an optical dust sensor has been shown to be able to capture most of the features of the $PM_{2.5}$ time series in a wood-smoke impacted area after suitable baseline and temperature corrections are applied.

In controlled conditions, the optical dust sensor used in ODIN was shown to have a stable baseline with a small dependence with ambient temperature. However, field data indicates a significant baseline drift and temperature interference. The baseline drift of nearly 30 % in three weeks indicates that regular checks will be required if the ODIN is to be used for extended periods of time.

The fact that the temperature interference observed in the field tests was more significant than that observed in lab conditions suggests that the changes in the response of the ODIN to ambient temperature are related to the nature of the aerosol sampled and not only to the sensor themselves. This has implications for the transferability of the correction factors to other locations.

Also, the performance of the ODIN is worst for $PM_{2.5}$ concentrations below 25 $\mu g\,m^{-3}$. This is to be expected as the datasheet of the Sharp dust sensor has a response curve starting at 100 $\mu g\,m^{-3}$. This is a common characteristic of low-cost sensors (Wang and Brauer, 2014) and one should be cautious when using these sensors in low-concentration environments as their response may reflect more their noise than a real measurement.

A simple test of the performance of ODIN against wind speed and direction found that the inlet performed as expected with no wind direction bias and only a small negative wind speed trend. This negative trend with wind speed may also be related to the

AMTD
8, 7511–7533, 2015
ODIN development and performance
G. Olivares and S. Edwards

fact that high wind speeds relate to low concentrations, where the Sharp dust sensor perform worst, and that a different source mix may be dominant in those conditions.

Nevertheless, the ODIN is shown to be a useful complement to regulatory measurements for campaigns and its calibration parameters are stable for deployments of around one month.

The next steps in understanding the response of the ODIN to urban aerosols are to explore more in detail the performance of the Sharp dust sensor to specific aerosol populations (size and composition), explore the inter-instrument variability and the drivers for the baseline drift and temperature interference found here. We also expect to explore the transferability of correction coefficients with data currently being captured in Auckland and Christchurch and it is expected to generate results by September 2015.

Future versions of the ODIN are expected to include distributed telemetry for high density deployments at a city scale as well as improved energy efficiency for long term deployments.

Acknowledgements. The development of ODIN was funded through NIWA's Atmosphere and Health 2013-14 programme (ATHS1301). The ODIN deployments and data analysis were funded through NIWA's Impacts of Air Pollutants 2014-15 programme (CAAP1504). Also, we gratefully acknowledge the support from Environment Canterbury through Teresa Aberkane in giving us access to Christchurch's air quality monitoring sites and data.

References

Aberkane, T., Harvey, M., and Webb, M.: Annual Ambient Air Quality Monitoring Report 2009, no. U04/58 in Environment Canterbury Technical Report, Environment Canterbury, Christchurch, available at: http://www.crc.govt.nz/publications/Reports/annual-ambient-air-quality-monitoring-report-2009-000310.pdf (last access: 8 Juy 2014), 2010. 7517, 7520

Adafruit: MicroSD Card Breakout Board+ ID: 254 – USD 14.95, Adafruit Industries, Unique & Fun DIY Electronics And Kits, available at: http://www.adafruit.com/products/254 (last access: 19 May 2015), 2014. 7515

AMTD
8, 7511–7533, 2015

ODIN development and performance

G. Olivares and S. Edwards

Air Quality Egg: Air Quality Egg, available at: http://airqualityegg.com/, last access: 4 July 2014. 7513
AOSONG: Aosong(Guangzhou) Electronics Co.,Ltd., available at: http://www.aosong.com/en/products/details.asp?id=117, last access: 19 May 2015. 7515
Asian Development Bank: Improving Air Quality Monitoring in Asia: a Good Practice Guidance, Tech. rep., Asian Development Bank, Mandaluyong City, Philippines, available at: http://cleanairasia.org/portal/sites/default/files/improving_aqmt_in_asia.pdf (last access: 19 May 2015), 2014. 7512
Brauer, M., Amann, M., Burnett, R. T., Cohen, A., Dentener, F., Ezzati, M., Henderson, S. B., Krzyzanowski, M., Martin, R. V., Van Dingenen, R., van Donkelaar, A., and Thurston, G. D.: Exposure assessment for estimation of the global burden of disease attributable to outdoor air pollution, Environ. Sci. Technol., 46, 652–660, doi:10.1021/es2025752, 2012. 7512
Carslaw, D. C. and Ropkins, K.: openair – an R package for air quality data analysis, Environ. Modell. Softw., 27–28, 52–61, doi:10.1016/j.envsoft.2011.09.008, 2012. 7517
Chow, J. C., Engelbrecht, J. P., Watson, J. G., Wilson, W. E., Frank, N. H., and Zhu, T.: Designing monitoring networks to represent outdoor human exposure, Chemosphere, 49, 961–978, doi:10.1016/S0045-6535(02)00239-4, 2002. 7512, 7513
Hart, J. K. and Martinez, K.: Environmental sensor networks: a revolution in the earth system science?, Earth-Sci. Rev., 78, 177–191, doi:10.1016/j.earscirev.2006.05.001, 2006. 7513
Holstius, D. M., Pillarisetti, A., Smith, K. R., and Seto, E.: Field calibrations of a low-cost aerosol sensor at a regulatory monitoring site in California, Atmos. Meas. Tech., 7, 1121–1131, doi:10.5194/amt-7-1121-2014, 2014. 7512, 7514
Lim, S. S., Vos, T., Flaxman, A. D., Danaei, G., Shibuya, K., Adair-Rohani, H., AlMazroa, M. A., Amann, M., Anderson, H. R., Andrews, K. G., Aryee, M., Atkinson, C., Bacchus, L. J., Bahalim, A. N., Balakrishnan, K., Balmes, J., Barker-Collo, S., Baxter, A., Bell, M. L., Blore, J. D., Blyth, F., Bonner, C., Borges, G., Bourne, R., Boussinesq, M., Brauer, M., Brooks, P., Bruce, N. G., Brunekreef, B., Bryan-Hancock, C., Bucello, C., Buchbinder, R., Bull, F., Burnett, R. T., Byers, T. E., Calabria, B., Carapetis, J., Carnahan, E., Chafe, Z., Charlson, F., Chen, H., Chen, J. S., Cheng, A. T.-A., Child, J. C., Cohen, A., Colson, K. E., Cowie, B. C., Darby, S., Darling, S., Davis, A., Degenhardt, L., Dentener, F., Des Jarlais, D. C., Devries, K., Dherani, M., Ding, E. L., Dorsey, E. R., Driscoll, T., Edmond, K., Ali, S. E., Engell, R. E., and Erwin, P. J., Fahimi, S., Falder, G., Farzadfar, F., Ferrari, A., Finucane, M. M., Flaxman, S., Fowkes, F. G. R., Freedman, G., Freeman, M. K., Gakidou, E., Ghosh, S., Gio-

AMTD
8, 7511–7533, 2015

ODIN development and performance

G. Olivares and S. Edwards

vannucci, E., Gmel, G., Graham, K., Grainger, R., Grant, B., Gunnell, D., Gutierrez, H. R., Hall, W., Hoek, H. W., Hogan, A., Hosgood, H. D., Hoy, D., Hu, H., Hubbell, B. J., Hutchings, S. J., Ibeanusi, S. E., Jacklyn, G. L., Jasrasaria, R., Jonas, J. B., Kan, H., Kanis, J. A., Kassebaum, N., Kawakami, N., Khang, Y.-H., Khatibzadeh, S., Khoo, J.-P., Kok, C., Laden, F., Lalloo, R., Lan, Q., Lathlean, T., Leasher, J. L., Leigh, J., Li, Y., Lin, J. K., Lipshultz, S. E., London, S., Lozano, R., Lu, Y., Mak, J., Malekzadeh, R., Mallinger, L., Marcenes, W., March, L., Marks, R., Martin, R., McGale, P., McGrath, J., Mehta, S., Memish, Z. A., Mensah, G. A., Merriman, T. R., Micha, R., Michaud, C., Mishra, V., Hanafiah, K. M., Mokdad, A. A., Morawska, L., Mozaffarian, D., Murphy, T., Naghavi, M., Neal, B., Nelson, P. K., Nolla, J. M., Norman, R., Olives, C., Omer, S. B., Orchard, J., Osborne, R., Ostro, B., Page, A., Pandey, K. D., Parry, C. D., Passmore, E., Patra, J., Pearce, N., Pelizzari, P. M., Petzold, M., Phillips, M. R., Pope, D., Pope, C. A., Powles, J., Rao, M., Razavi, H., Rehfuess, E. A., Rehm, J. T., Ritz, B., Rivara, F. P., Roberts, T., Robinson, C., Rodriguez-Portales, J. A., Romieu, I., Room, R., Rosenfeld, L. C., Roy, A., Rushton, L., Salomon, J. A., Sampson, U., Sanchez-Riera, L., Sanman, E., Sapkota, A., Seedat, S., Shi, P., Shield, K., Shivakoti, R., Singh, G. M., Sleet, D. A., Smith, E., Smith, K. R., Stapelberg, N. J., Steenland, K., Stöckl, H., Stovner, L. J., Straif, K., Straney, L., Thurston, G. D., Tran, J. H., Van Dingenen, R., van Donkelaar, A., Veerman, J. L., Vijayakumar, L., Weintraub, R., Weissman, M. M., White, R. A., Whiteford, H., Wiersma, S. T., Wilkinson, J. D., Williams, H. C., Williams, W., Wilson, N., Woolf, A. D., Yip, P., Zielinski, J. M., Lopez, A. D., Murray, C. J., and Ezzati, M.: A comparative risk assessment of burden of disease and injury attributable to 67 risk factors and risk factor clusters in 21 regions, 1990–2010: a systematic analysis for the Global Burden of Disease Study 2010, Lancet, 380, 2224–2260, doi:10.1016/S0140-6736(12)61766-8, 2012. 7512

Macetech: chronodot_v2.0, macetech documentation, available at: http://docs.macetech.com/doku.php/chronodot%5C_v2.0 (last access: 19 May 2015), 2013. 7516

Maks, S.: Stephanie-Maks/Arduino-Chronodot, available at: https://github.com/Stephanie-Maks/Arduino-Chronodot (last access: 1 May 2015), 2012. 7516

McKone, T. E., Ryan, P. B., and Özkaynak, H.: Exposure information in environmental health research: current opportunities and future directions for particulate matter, ozone, and toxic air pollutants, J. Expo. Sci. Env. Epid., 19, 30–44, doi:10.1038/jes.2008.3, 2008. 7512

Olivares, G.: ODIN Test and Co-Location Data, available at: http://figshare.com/articles/ODIN_test_and_co_location_data/1439794 (last access: 15 June 2015), 2015a. 7517

AMTD

8, 7511–7533, 2015

ODIN development and performance

G. Olivares and S. Edwards

Olivares, G.: ODIN Analysis Script June 2015, available at: http://figshare.com/articles/ODIN_analysis_script_June_2015/1449236 (last access: 15 June 2015), 2015b. 7517
Olivares, G. and Edwards, S.: ODIN Firmware, doi:10.6084/m9.figshare.1094459, 2014. 7514, 7515, 7527
Olivares, G., Longley, I., and Coulson, G.: Development of a Low-Cost Device for Observing Indoor Particle Levels Associated With Source Activities in the Home, available at: http://figshare.com/articles/Development_of_a_low_cost_device_for_observing_indoor_particle_levels_associated_with_source_activities_in_the_home/646186 (last access: 27 August 2014), 2013. 7514, 7518, 7519
SHARP: GP2Y1010AU0F – Air Sensor, Sharp Microelectronics Europe, available at: http://www.sharpsme.com/optoelectronics/sensors/air-sensors/GP2Y1010AU0F, last access: 19 May 2015. 7515
Smith, P. and Clark, M.: Microsampling Air Pollution, available at: http://well.blogs.nytimes.com/2013/06/03/microsampling-air-pollution/ (last access: 19 May 2015), 2013. 7513
Snyder, E. G., Watkins, T. H., Solomon, P. A., Thoma, E. D., Williams, R. W., Hagler, G. S. W., Shelow, D., Hindin, D. A., Kilaru, V. J., and Preuss, P. W.: The changing paradigm of air pollution monitoring, Environ. Sci. Technol., 47, 11369–11377, doi:10.1021/es4022602, 2013. 7512, 7513
Sparkfun: Arduino Pro Mini 328 – 5 V/16 MHz – DEV-11113, SparkFun Electronics, available at: https://www.sparkfun.com/products/11113 (last access: 19 May 2015), 2014. 7515
SPECK: Speck™, available at: https://www.specksensor.com/, last access: 19 May 2015. 7513
Team, R. C.: R: a Language and Environment for Statistical Computing, available at: http://www.R-project.org/, last access: 9 July 2014. 7517
Wang, A. and Brauer, M.: Review of Next Generation Air Monitors for Air Pollution, available at: https://circle.ubc.ca/handle/2429/46628 (last access: 19 May 2015), 2014. 7513, 7520
Williams, R., Kaufman, A., Hanley, T., Rice, J., and Garvey, S.: Evaluation of Field-deployed Low Cost PM Sensors, Tech. Rep. EPA/600/R-14/464, U.S. EPA, available at: http://www.epa.gov/heasd/images/PM%20Sensor%20Evaluation%20Report%20EPA-600-R-14-464.pdf (last access: 19 May 2015), 2014. 7514
Wilson, J. G., Kingham, S., Pearce, J., and Sturman, A. P.: A review of intraurban variations in particulate air pollution: implications for epidemiological research, Atmos. Environ., 39, 6444–6462, doi:10.1016/j.atmosenv.2005.07.030, 2005. 7512, 7513

AMTD
8, 7511–7533, 2015

ODIN development and performance

G. Olivares and S. Edwards

Table 1. Results from the dust sensor baseline experiment where eight Sharp dust sensors were placed in a clean, temperature controlled environment.

Metric	Dust1	Dust2	Dust3	Dust4	Dust5	Dust6	Dust7	Dust8
Mean (mV)	0.24	0.99	28.0	0.96	8.70	4.50	11.0	11.0
SD (mV)	0.15	0.30	0.91	0.28	0.37	0.30	0.40	0.45
Median (mV)	0.21	0.94	28.0	0.94	8.70	4.50	11.0	11.0
Minimum (mV)	0.00	0.21	25.0	0.21	7.30	3.60	9.80	9.40
Maximum (mV)	0.73	1.80	30.0	2.00	9.70	5.50	12.0	12.0
Observations	678	678	678	678	678	678	678	678

AMTD
8, 7511–7533, 2015

G. Olivares and S. Edwards

Table 2. Details of the corrections applied to the data. The error estimates correspond to the 95 % confidence interval of the coefficients. The RMSE and R^2 correspond to the whole dataset estimates.

Correction	Expression	Notes
Baseline	Initial: 403 mV Drift: −0.22 mV h^{-1}	
Temperature	ODIN = (−4.4 ± 0.5) · Temperature (−49 ± 8)	
Calibration	$PM_{2.5}$ = (0.6 ± 0.04) · ODIN + (19 ± 2)	RMSE = 14.1 µg m^{-3} R^2 = 0.72

AMTD
8, 7511–7533, 2015

G. Olivares and S. Edwards

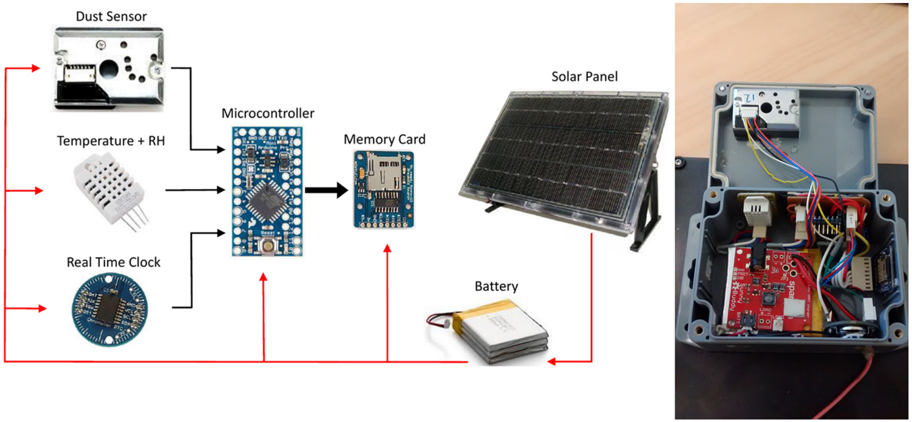

Figure 1. Internal layout and simplified diagram of ODIN showing the main components and the flow of power (red arrows) and information (black arrows). The picture on the right shows how the components fit inside the enclosure with the dust sensor attached to the lid of the unit and exposed through a hole directly over its sensing area. See Olivares and Edwards (2014) for the full electrical schematics.

AMTD
8, 7511–7533, 2015

G. Olivares and S. Edwards

Title Page
Abstract | Introduction
Conclusions | References
Tables | Figures
◀| |▶
◀ ▶
Back | Close
Full Screen / Esc
Printer-friendly Version
Interactive Discussion

Figure 2. Deployment of ODIN_01 at ECan's air quality monitoring site. The circles show the location of the unit attached to the meteorological mast.

AMTD
8, 7511–7533, 2015

ODIN development and performance

G. Olivares and S. Edwards

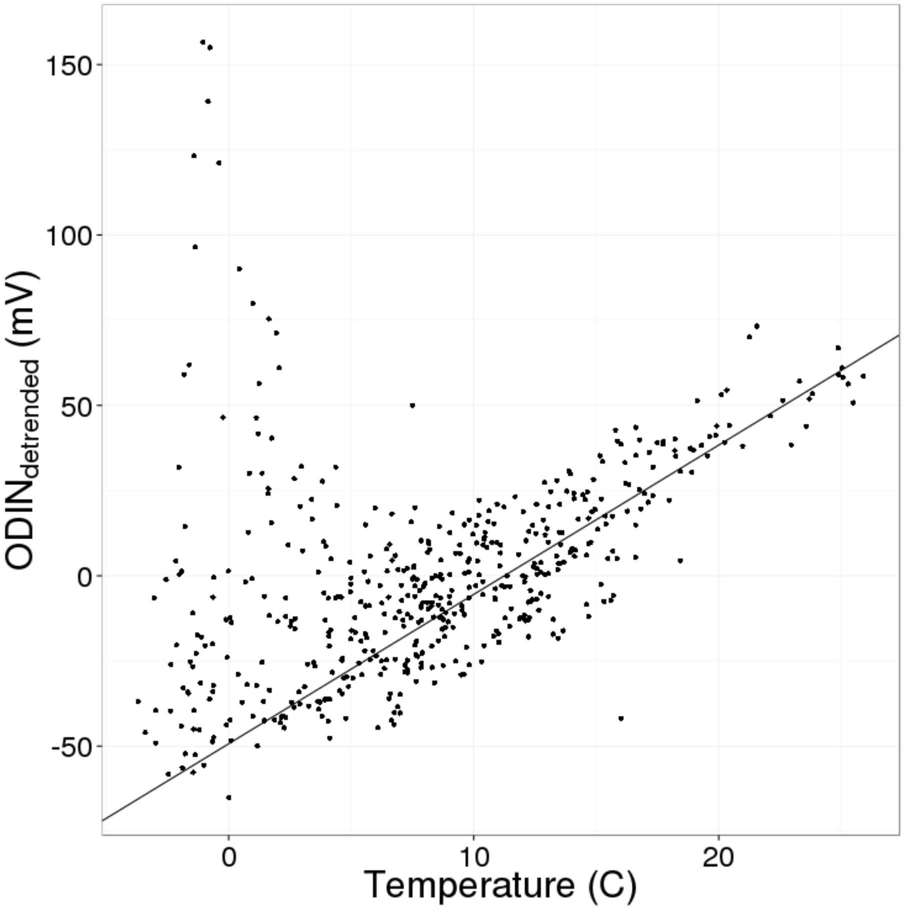

Figure 3. Scatter plot of the baseline corrected ODIN data against instrument temperature. The full line corresponds to the estimated temperature correction based on these data.

AMTD
8, 7511–7533, 2015

ODIN development and performance

G. Olivares and S. Edwards

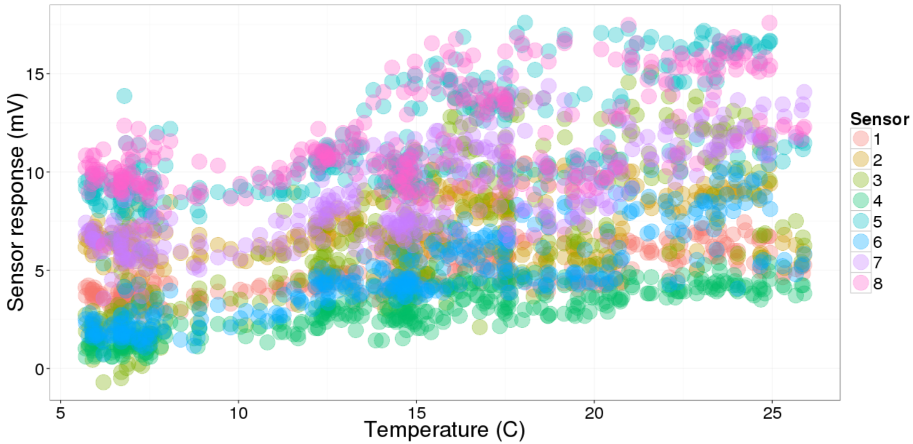

Figure 4. Scatter plot of one minute dust sensor data (mV) against temperature (°C). Colour indicates the different units.

AMTD
8, 7511–7533, 2015

ODIN development and performance

G. Olivares and S. Edwards

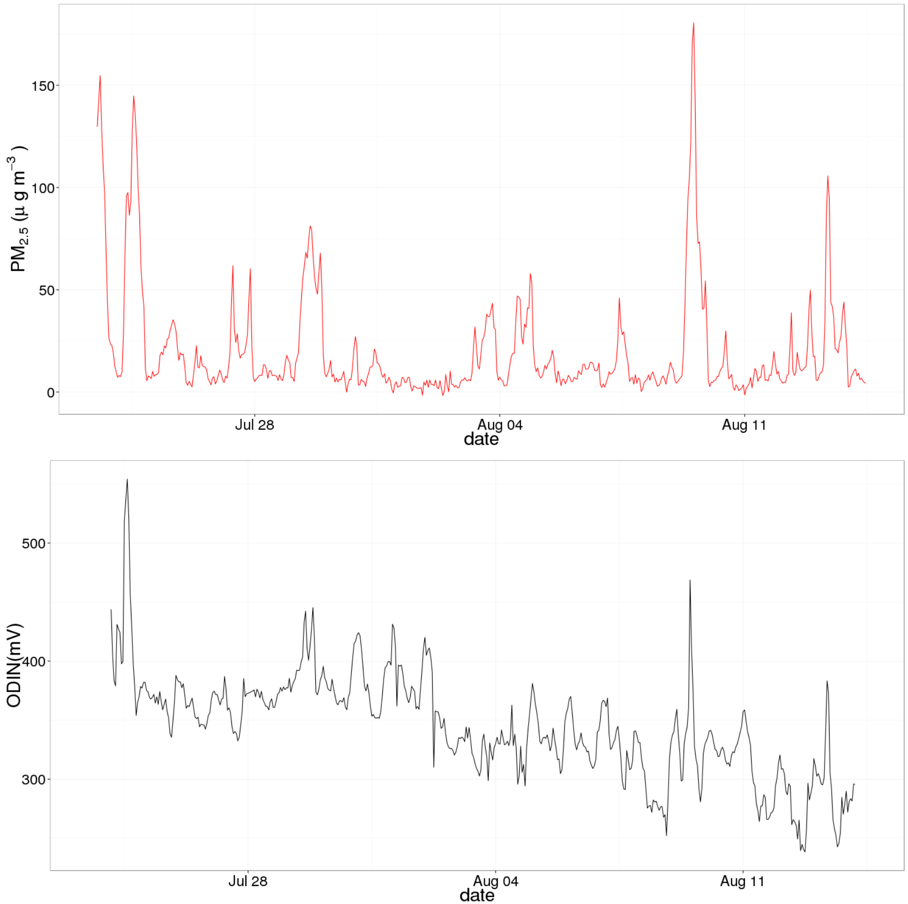

Figure 5. Hourly time series of $PM_{2.5}$ (top plot) and raw output from ODIN (bottom plot) highlighting the significant drift in the ODIN's baseline. Note the different units of the ODIN raw response and the different scales on the plots.

AMTD
8, 7511–7533, 2015

ODIN development and performance

G. Olivares and
S. Edwards

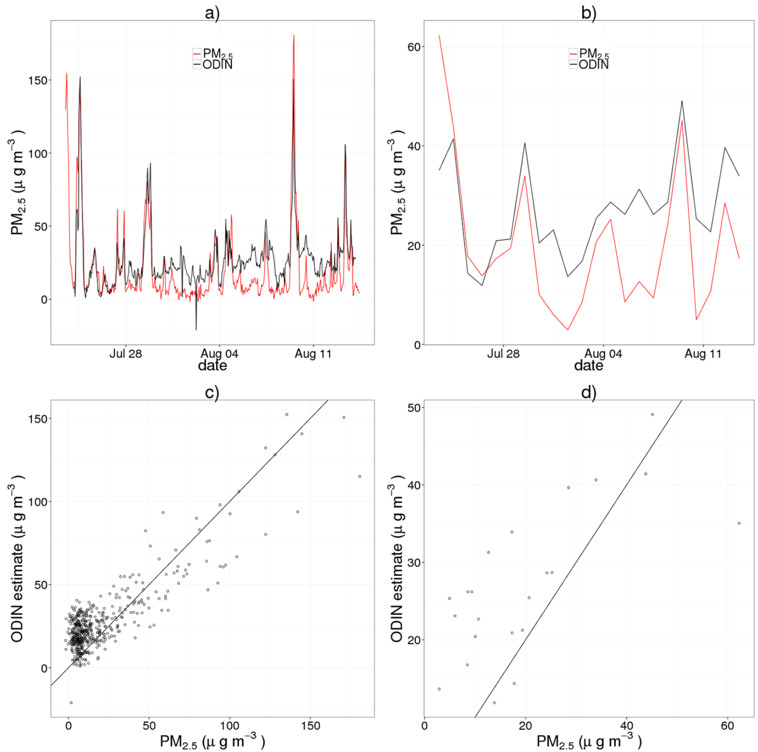

Figure 6. Comparison between the standard measurements. Panel **(a)** shows the hourly time series of $PM_{2.5}$ and the calibrated ODIN data. Panel **(b)** shows the equivalent daily time series. Panels (**c** and **d**) show the scatter plots of for the hourly and daily data with the black lines indicating the 1 : 1 line.

AMTD
8, 7511–7533, 2015

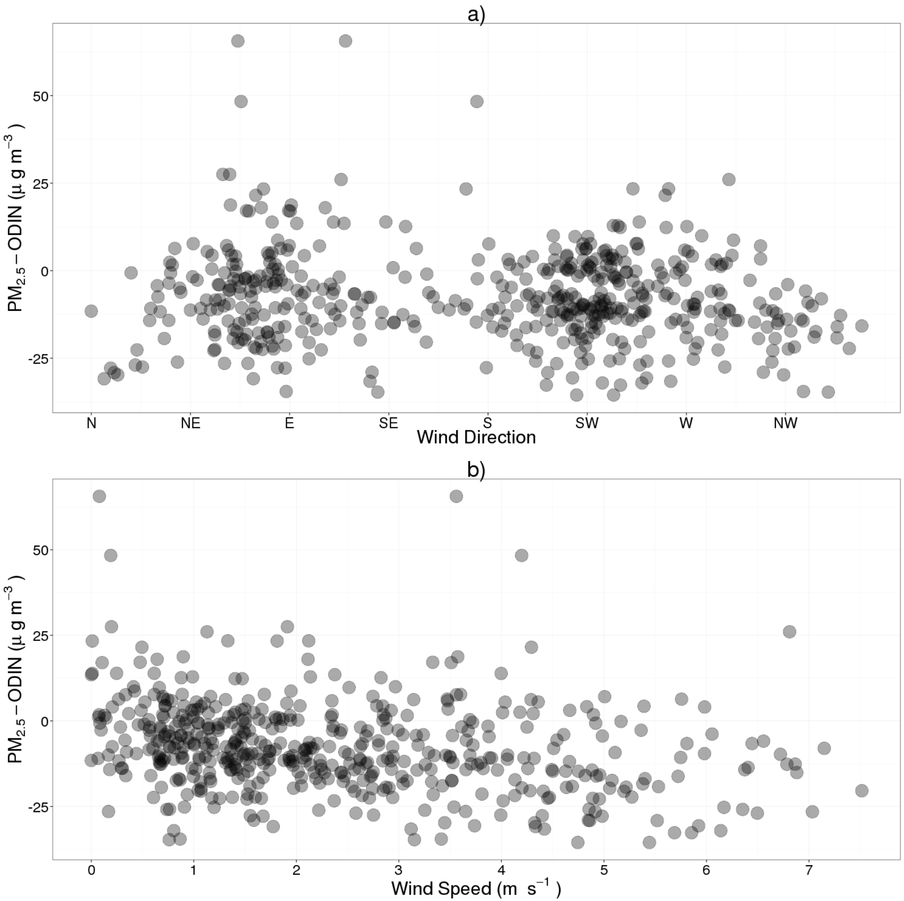

Figure 7. Comparison between the error in the ODIN $PM_{2.5}$ estimate as a function of wind direction **(a)** and wind speed **(b)**. The error estimate is calculated as hourly values of $PM_{2.5}$ – ODIN.

AMTD
8, 7511–7533, 2015

ODIN development and performance

G. Olivares and S. Edwards